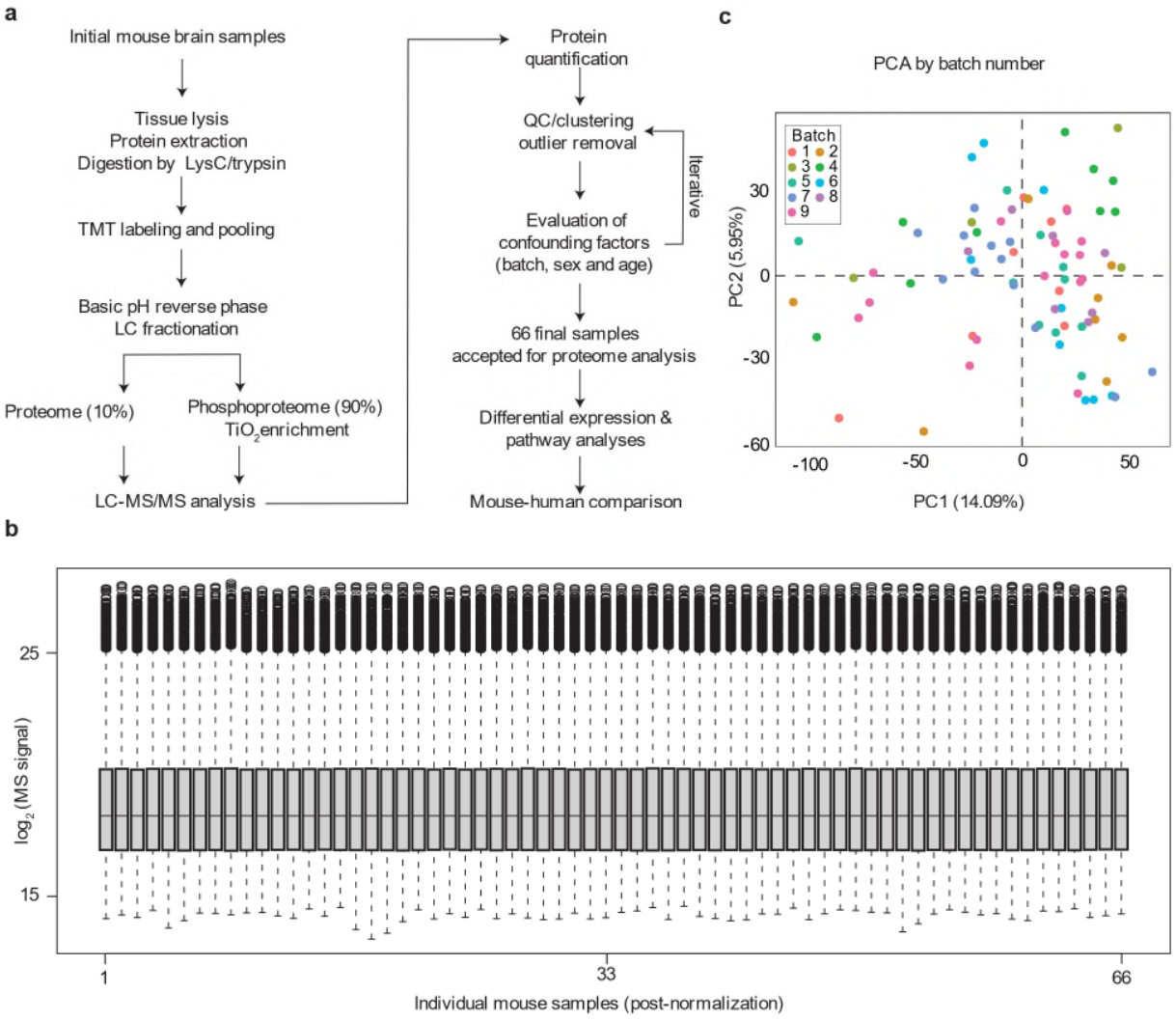

Supplementary Fig. 1 | Workflow and quality control of mouse proteomic samples. a, TMT-LC/LC-MS/MS and quality control workflow for analysis. Finally, 66 mouse samples were used in our proteome analysis. **b**, Box plot to show the distribution of normalized protein intensities in the mouse samples. **c**, Principal component analysis of mouse samples in different TMT batches. No batch bias was observed.

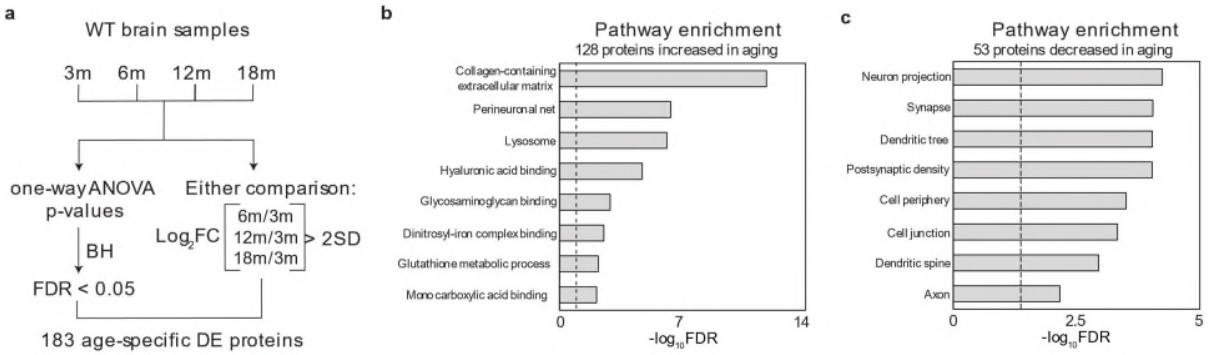

Supplementary Fig. 2 | Proteomic analysis of age-linked alterations in WT mice. a, Workflow of age-linked proteomics analysis. **b**, The cluster of upregulated proteins with age. Each line represents one protein. **c**, The cluster of downregulated proteins with age.

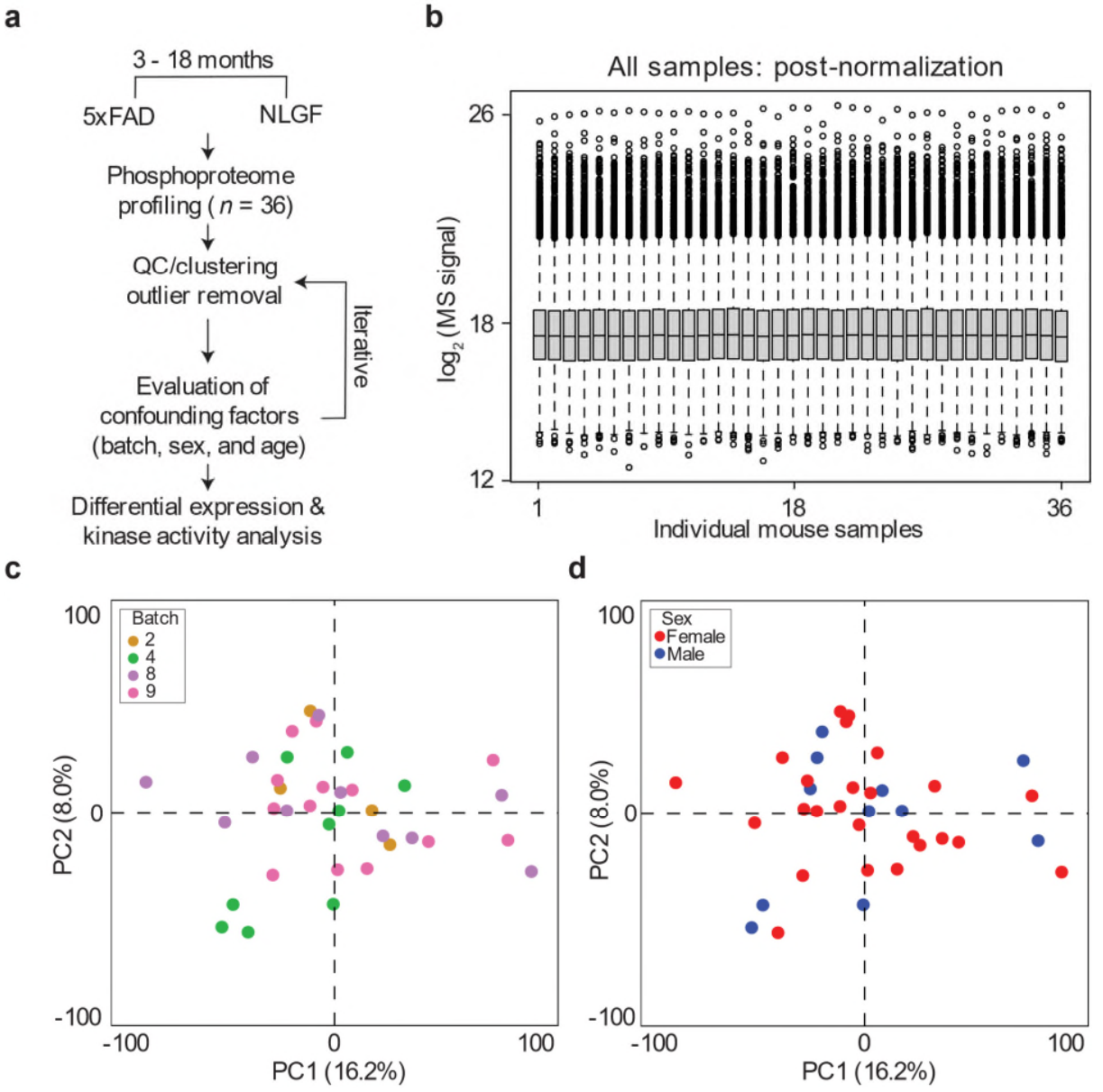

Supplementary Fig. 3 | Phosphoproteomic and quality control analysis of 5xFAD, NLGF and WT mice. **a**, Workflow for phosphoproteomics analysis. **b**, Distribution of measured phosphoprotein intensities in mouse samples. **c**, Principal component analysis of mouse samples highlighting the normalization of batch. **d**, Principal component analysis of mouse samples showing no obvious sex effect.

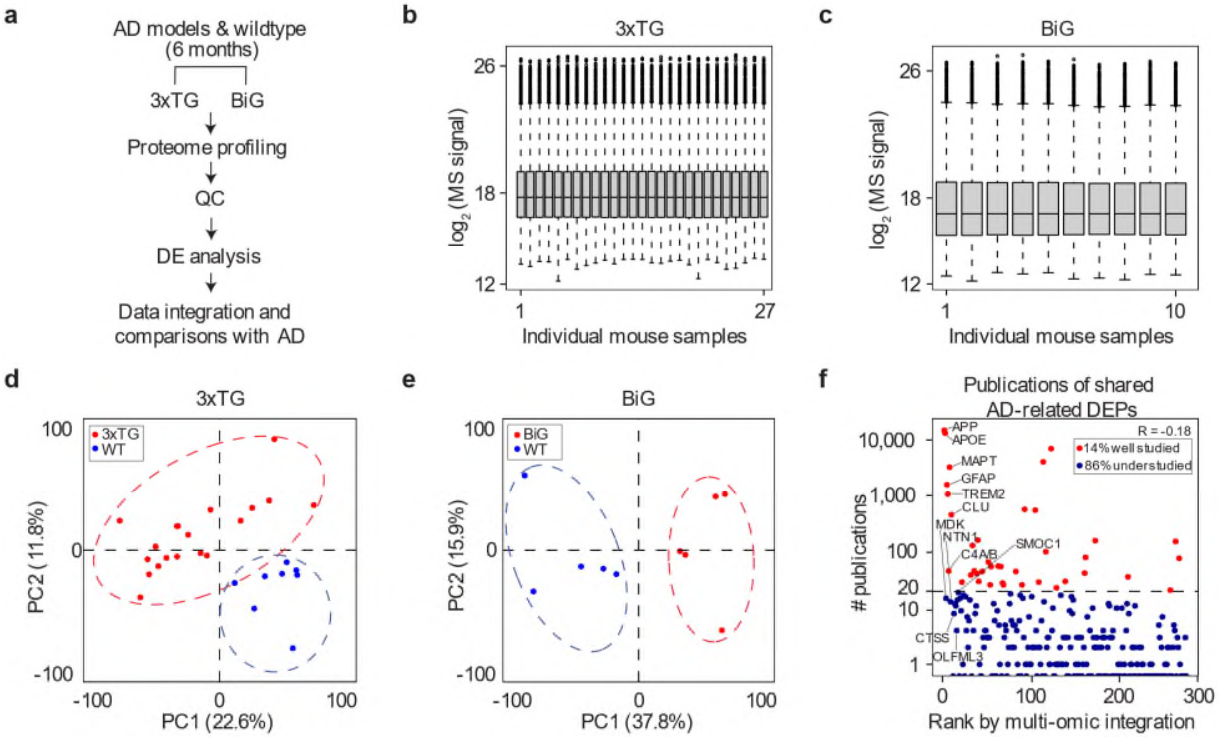

Supplementary Fig. 4 | Whole proteome analysis of 3xTG, BiG and WT mice and the publication record of the AD-mouse shared proteins. a, Workflow for whole proteome analysis by TMT-LC/LC-MS/MS. **b**, Distribution of normalized protein intensities in 3xTG and WT samples. **c**, Distribution of normalized protein intensities in BiG and WT samples. **d**, Principal component analysis of 3xTG and WT samples highlighting the difference between genotypes. **e**, Principal component analysis of BiG and WT samples highlighting the difference between genotypes. **f**, Publication record for the 275 AD-mouse shared proteins is represented by the number of publications and their integrative ranks determined by multi-omics analysis. The number of publications were found by PubMed search using “Alzheimer” and protein/gene names in August 2024. Using 20 publications as the cutoff, 14% of the proteins are well-studied, whereas 86% are under-researched. Notably, Pearson correlation analysis between the rank number and publication count yielded a negative value, suggesting that published research is disproportionately focused on a few well-known AD genes/proteins.

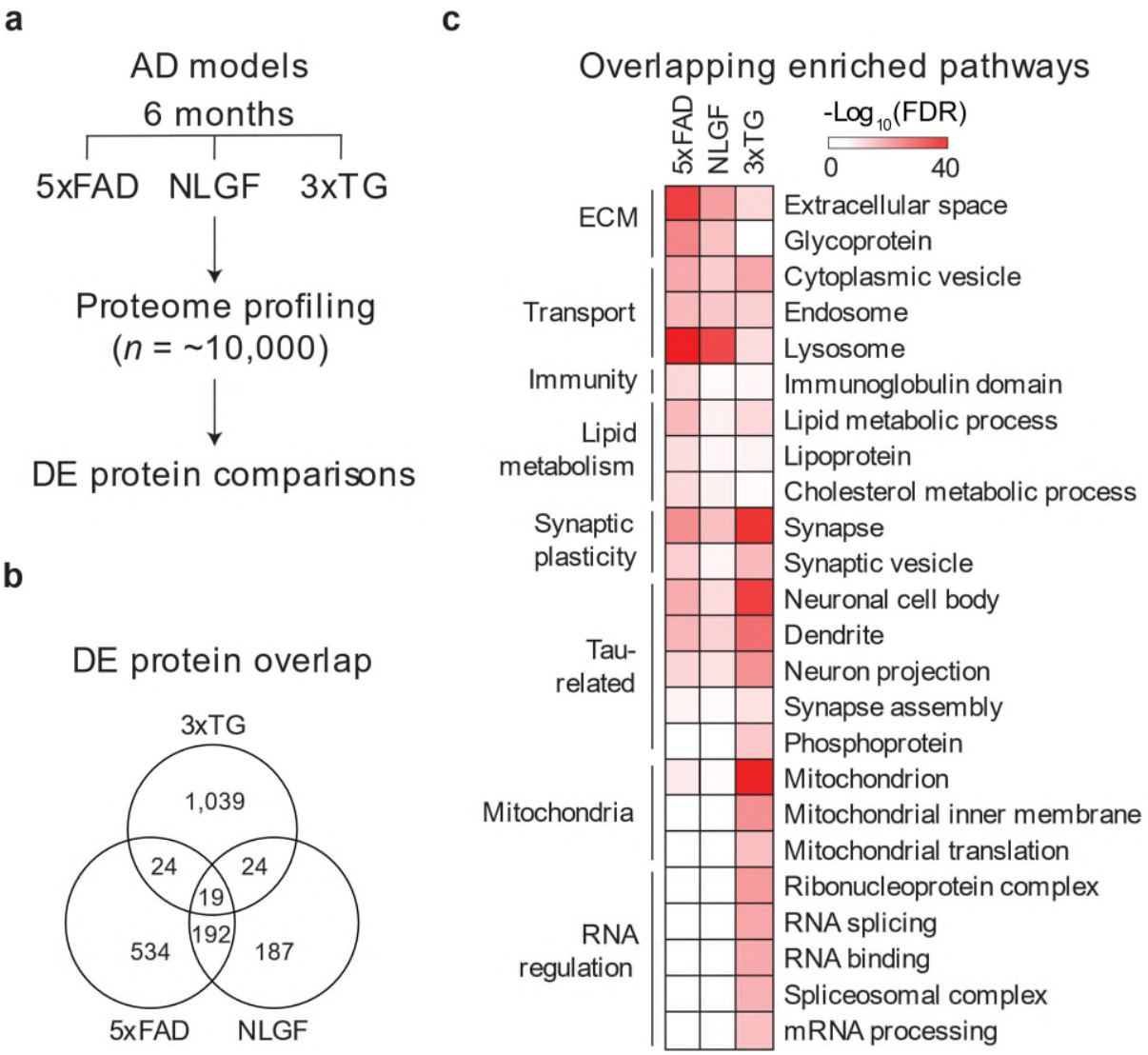

Supplementary Fig. 5 | Differential expression and pathway analysis in 5xFAD, NLGF, and 3xTG mouse models. a, Schematic of the workflow used to compare DE proteins across mouse models. **b**, Venn diagram illustrating the overlap of DE proteins in 5xFAD, NLGF, and 3xTG mice at 6 months of age. **c**, Pathway enrichment analysis showing biological pathways shared among models or uniquely enriched in 3xTG mice.

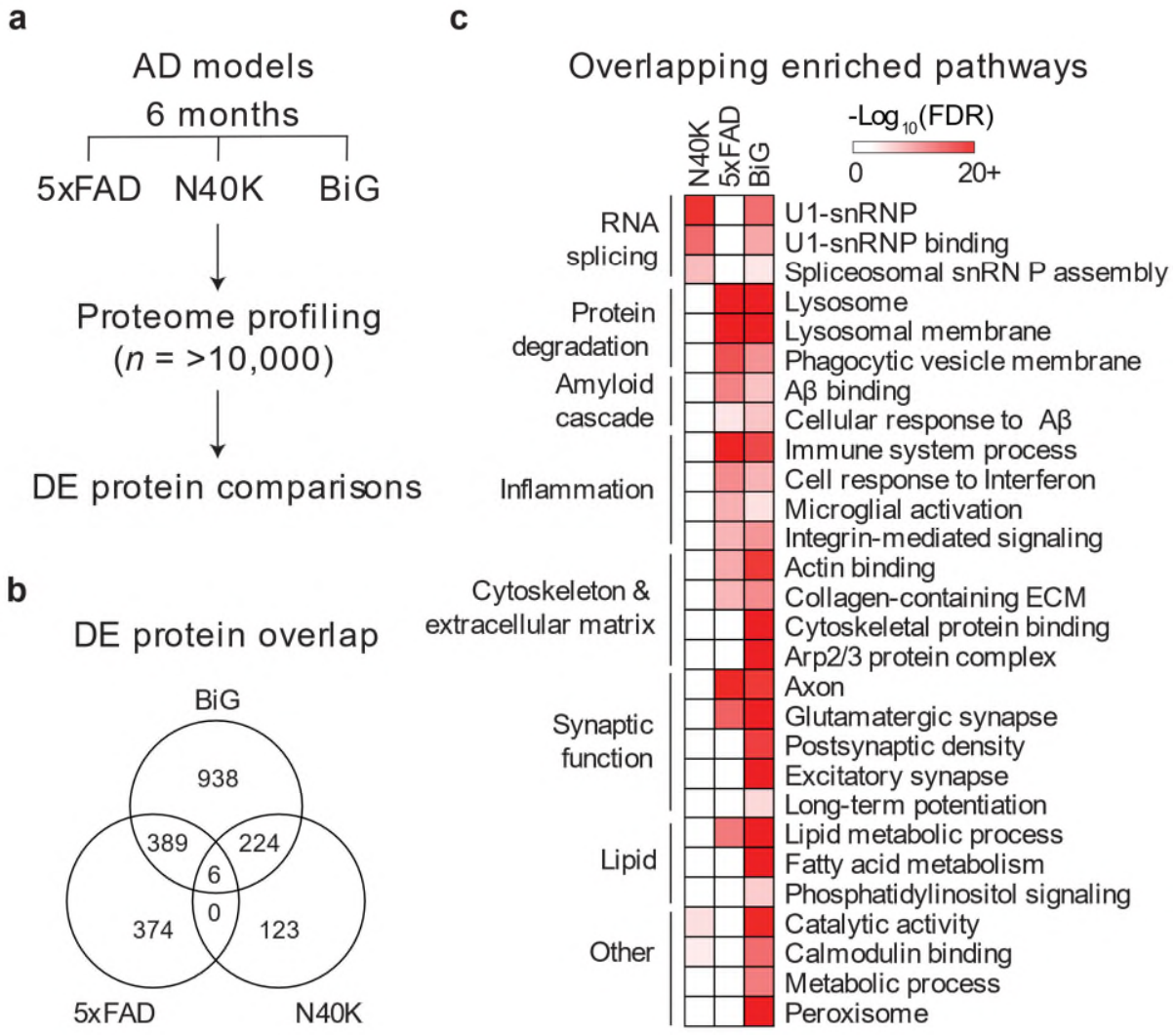

Supplementary Fig. 6 | Differential expression and pathway analysis in N40K, 5xFAD, and BiG mouse models. a, Schematic of the workflow used to compare DE proteins across mouse models. **b**, Venn diagram illustrating the overlap of DE proteins in N40K, 5xFAD, and BiG mice at 6 months of age. **c**, Pathway enrichment analysis showing pathways shared among models or synergistically enriched in BiG mice.

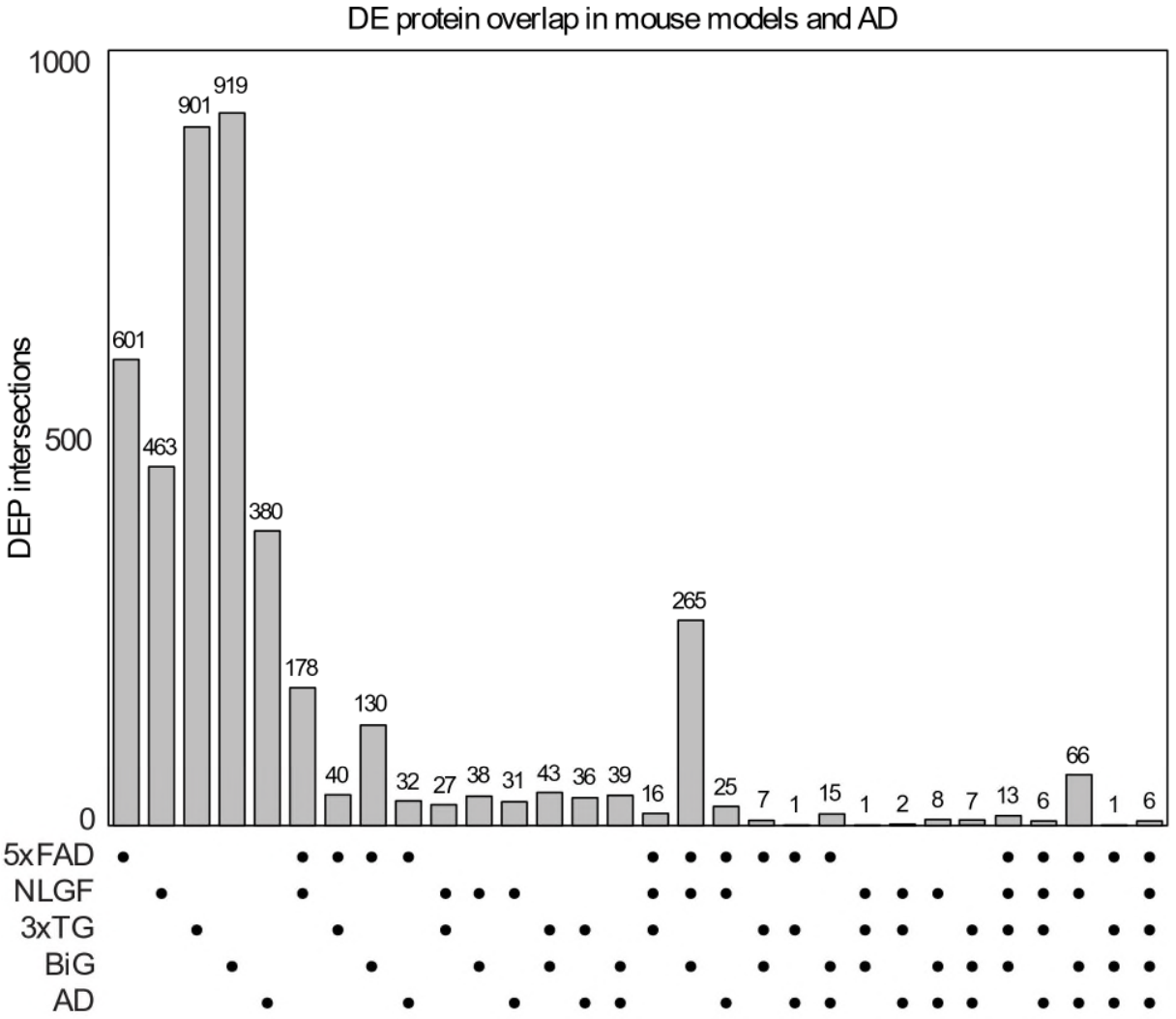

Supplementary Fig. 7 | Upset plot of all DE overlaps between mouse models and human AD. An upset plot depicting all DE protein overlaps across four mouse models and human AD. Dots indicate shared DE proteins among the specified groups, while the bar heights represent the size of each overlap.

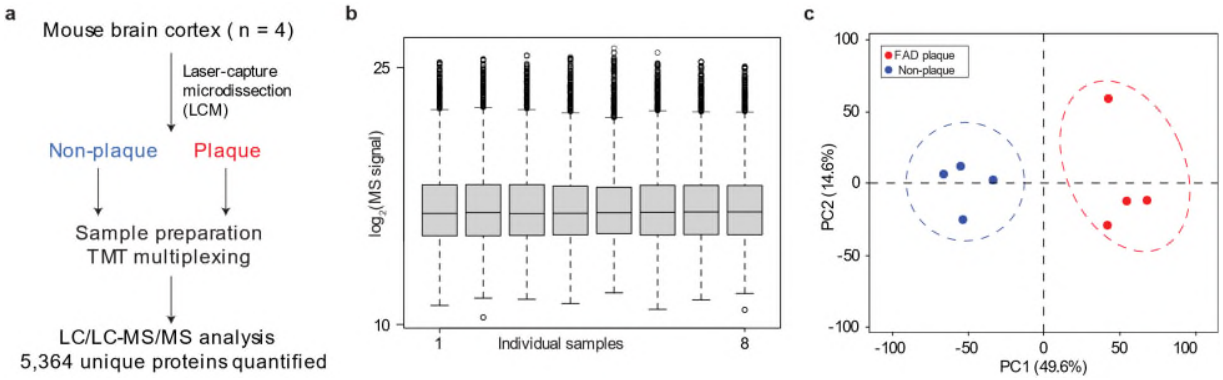

Supplementary Fig. 8 | Plaque proteome analysis of AD mice. a, Workflow for amyloid plaque isolation and proteome profiling by LCM-TMT-LC/LC-MS/MS. **b**, Distribution of normalized protein intensities in plaque and non-plaque samples. **c**, Principal component analysis highlighting the clear difference between the plaque and non-plaque results.

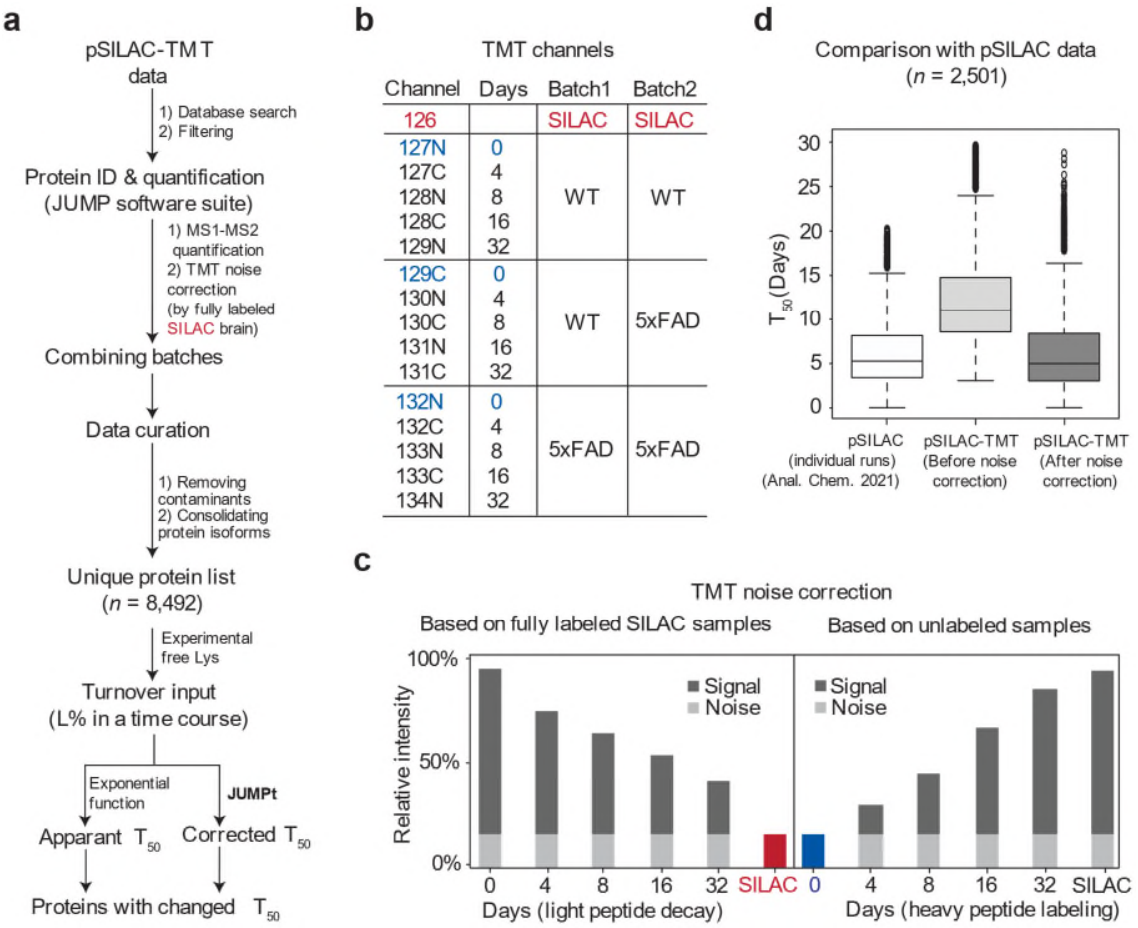

Supplementary Fig. 9 | Comprehensive workflow for mouse pSILAC-TMT-LC/LC-MS/MS analysis and the importance of TMT noise correction. a, Workflow including mouse pSILAC labeling, TMT-LC/LC-MS/MS experiments, protein identification and quantification via JUMP, batch merging, data curation, and JUMPt analysis for both apparent and corrected T50 turnover rates. **b**, TMT channels for proteomics experiments designed to include three replicates each of WT and 5xFAD mice, with five-time points (0, 4, 8, 16, and 32 days) distributed across two batches. The fully SILAC-labeled mouse brain tissues from two mouse generations[109] were highlighted in red, serving as a basis for noise correction. **c**, Schematic diagram illustrating the correction of TMT noise. In the light peptide decay curve, the fully labeled SILAC sample (red) facilitated noise detection since all Lys peptides were in the heavy form. Conversely, for the heavy peptide decay curve, the unlabeled sample (blue) from day 0 was utilized to determine the noise level. **d**, Comparison of protein half-lives in WT brain samples using the pSILAC and pSILAC-TMT methods. We used the same set of ~9-month-old mice to generate two datasets: (i) 3,260 proteins analyzed by pSILAC, where each labeling sample was analyzed independently. This smaller dataset was previously published in the JUMPt method paper [73]. (ii) 8,492 proteins analyzed by pSILAC-TMT, where all labeling samples were analyzed together in a hyperplexed TMT analysis. For the comparison between the two methods, we focused on the 2,501 overlapping proteins. In the pSILAC method, each sample was analyzed individually using the traditional approach, effectively avoiding ratio compression in the dataset. In contrast, the pSILAC-TMT method experienced ratio compression, resulting in significantly higher global protein half-lives compared to the traditional pSILAC analysis. However, after applying TMT noise correction, the half-lives in the two datasets aligned closely, demonstrating that the TMT noise was effectively mitigated.

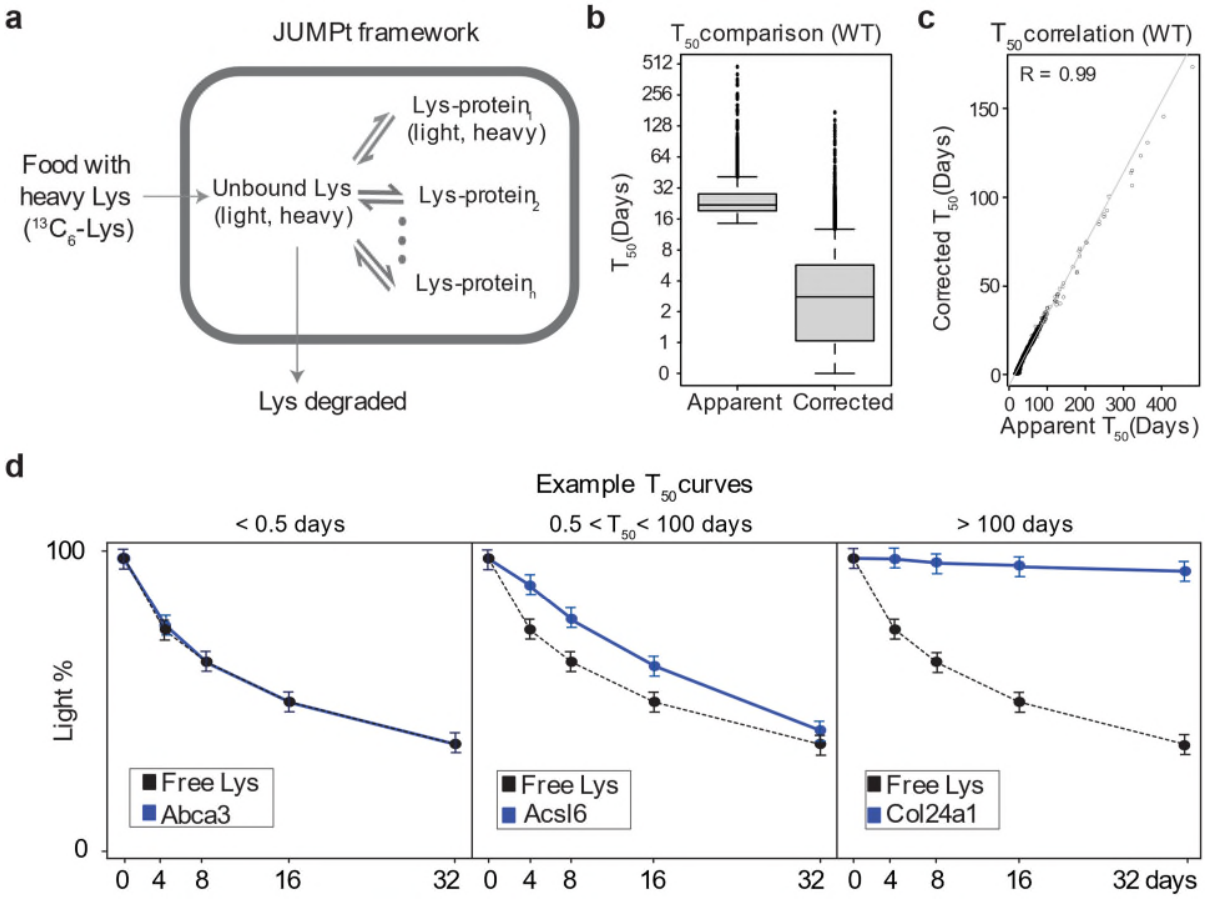

Supplementary Fig. 10 | The principle of half-life analysis by JUMPt considering the recycling of Lys in mice. a, Kinetic model for the JUMPt program: Heavy Lys is absorbed from food and transported into cells, contributing to a mixed pool containing previous light and newly absorbed heavy Lys. A portion of the Lys in cells is degraded, while the remainder is incorporated into proteins. When proteins degrade, the Lys in proteins is recycled back into the free Lys pool. **b**, The differences between apparent and corrected half-lives. **c**, Correlation between apparent and corrected half-lives. **d**, Examples of proteins with very short, intermediate, and very long half-lives: Proteins with very short half-lives have decay curves nearly overlapping with the free Lys curve, complicating accurate half-life calculation. These half-life values were set below 0.5 days. Conversely, proteins that decay very slowly have extremely long half-lives, presenting challenges for accurate computation. These half-life values were set above 100 days.

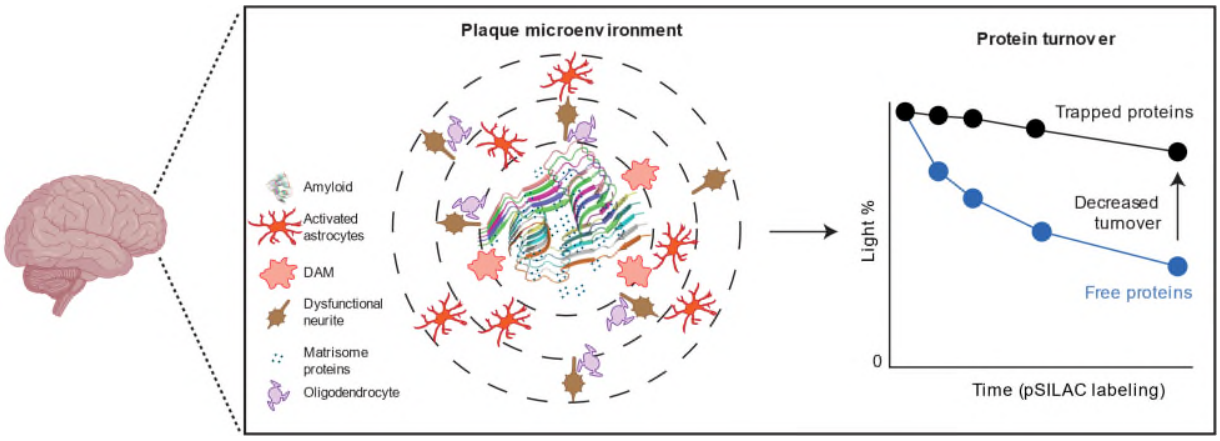

Supplementary Fig. 11 | Model showing components plaque microenvironment and the changes in protein turnover in amyloid plaque microenvironments. The core-shell model of plaque microenvironment is adapted from published spatial omics data[92]. The brain image created in BioRender. Yarbro, J. (2025) https://BioRender.com/a05v379.